Journal of Fluorine Chemistry 131 (2010) 635–641

Contents lists available at ScienceDirect

Journal of Fluorine Chemistry

journal homepage: www.elsevier.com/locate/fluor

Adsorption of fluoride on synthetic siderite from aqueous solution

Qiong Liu, Huaming Guo *, Yue Shan

School of Water Resources and Environment, China University of Geosciences, Beijing 100083, PR China

ARTICLE INFO

Article history:
Received 14 November 2009
Received in revised form 5 February 2010
Accepted 18 February 2010
Available online 24 February 2010

Keywords:
Groundwater
F^-
Removal
Kinetics
Thermodynamics

ABSTRACT

The study has investigated the feasibility of using synthetic siderite for F^- removal from aqueous solution. Batch experiments were performed to test effects of adsorbent dosage, contact time, initial F^- concentration, temperature, solution pH, and coexisting anions on F^- removal. Results show that the kinetic rate of F^- adsorption was high in the first 2 h, and thereafter significantly decreased. The kinetic data was better fitted to the pseudo-second order kinetic model than the pseudo-first order kinetic model. In comparison with Langmuir isotherm, both Freundlich and Redlich–Peterson isotherms better described the adsorption process, which indicates that the multilayer adsorption should be involved in the process of F^- removal. Thermodynamic study manifests that F^- adsorption on synthetic siderite was spontaneous and exothermic in nature. The synthetic siderite had high adsorption capacity for F^- removal, which was up to 1.775 mg/g in the batch with an adsorbent dosage of 5 g/L and an initial F^- concentration of 20 mg/L at 25 °C. The adsorption was relatively independent on solution pH between 4 and 9. The presence of Cl^- and NO_3^- had less impact on F^- adsorption, while PO_4^{3-} significantly affected F^- removal from aqueous solution. Results of X-ray diffraction (XRD) and scanning electron microscopy (SEM) suggest that the high adsorption capacity possibly arose from both coprecipitation of ferric hydroxide with F^- and adsorption of F^- on the fresh goethite.

© 2010 Elsevier B.V. All rights reserved.

1. Introduction

High F^- groundwaters have been found in more than 20 developed and developing countries, including China, India, Korea, Russia, Sri Lanka, Pakistan, Argentina and Mexico [1,18–21], which would result from both natural processes and human activities [2,3]. Although small amounts of F^- in ingested water are considered good to dental caries, particularly among children [4], excessive intake of F^- causes dental or skeletal fluorosis, which is a chronic, progressive disease manifested by mottling of teeth in mild cases and softening of bones or neurological damage in severe cases [3]. In order to protect public health, World Health Organization (WHO) has set the guideline level for F^- in drinking water at 1.5 mg/L [5]. The safe limit of F^- concentration in drinking water is 1.0 mg/L in China [6]. Therefore, it is very necessary to remove excess F^- from drinking water using an effective and robust technique.

Fluoride removal from drinking water can be achieved by adsorption, ion-exchange, precipitation-coagulation, membrane separation, electric methods (i.e., electrodialysis, eletrocoagulation and eletrocoagulation flota, etc.) [1,7–9]. Among those technologies, adsorption and coagulation are believed to be the cheapest methods. Although coagulation with iron and aluminium salts is more effective, the requirement of skilled operator and the introduction of contaminants into the water limit its application in small community and household levels. Since solid adsorbents are easy to handle and are appropriate for use in country side where high F^- groundwater mostly occurs, adsorption has received much attention on F^- removal. Iron/aluminium containing adsorbents have been widely used for F^- removal from aqueous solution, due to their high specific surface area, including hydrous iron(III)–tin(IV) bimetal mixed oxide[3], granular ferric hydroxide [11], mesoporous alumina [12], ferric(III) hydroxide-activated iron-manganese nodules [13], activated aluminium oxide [10,14], and polymer/alumina composites [15]. However, no studies have focused on F^- removal using synthetic siderite, although it was reported that the synthetic siderite has high adsorption capacity and good adsorption kinetics for removal of As oxyanions [16].

In this study, the defluoridation feasibility of synthetic siderite has been investigated by means of batch method. The main objectives are (i) to reveal the F^- adsorption kinetics, (ii) to assess the impact of initial F^- concentration, temperature, pH and coexisting anions on F^- removal kinetics and/or capacities; and (iii) to describe some important thermodynamic characteristics.

2. Materials and methods

2.1. Materials

All chemicals used were of reagent grade. Stock F^- solution (100 mg F^-/L) was prepared from sodium fluoride (A.R.) using

* Corresponding author. Tel.: +86 10 8232 1366; fax: +86 10 8232 1081.
E-mail address: hmguo@cugb.edu.cn (H. Guo).

0022-1139/$ – see front matter © 2010 Elsevier B.V. All rights reserved.
doi:10.1016/j.jfluchem.2010.02.006

deionized water. All glasswares and sample bottles were rinsed with 10% HNO_3 for at least 24 h, soaked with tap water, and finally rinsed with deionized water three times.

Synthetic siderite was precipitated by mixing 1 M Fe^{2+} with 2 M HCO_3^- at room temperature. The precipitate was filtered with 0.45 μm membrane. After rinsed with deionized water for three times, the artificial siderite was put onto an evaporation pan at room temperature for 48 h. After dried, oxidized part mainly presented on the surface was discarded. The inner part without being oxidized was crushed into powder (200 mesh), and kept in a desiccator. The powder was used as adsorbent for F^- removal in this study.

2.2. Batch experiments

The batch experiments were carried out by reacting 50 mL of F^- solution in 100 mL polyethylene bottles with the adsorbent. Unless otherwise specified, solution having pH 6.86 was used for adsorption experiments. The batch bottles were kept in a shaking water bath with a thermostatic controller at specified temperature for a predetermined contact time. The shaker speed was 150 rpm. After a predetermined contact time, the supernatant was decanted, centrifuged and filtered with 0.45 μm cellulose acetate membranes, and analyzed for residual F^- concentrations.

Effect of adsorbent dosage was investigated with initial F^- concentration of 20 mg/L, contact time of 8 h, and adsorbent dosages between 4 and 40 g/L at 25 °C. Effect of contact time (10 min–12 h) was examined at 25 °C with initial F^- concentrations of 3.0 and 10.0 mg/L, respectively. Adsorption isotherm studies were conducted with initial F^- concentrations between 3 and 20 mg/L at different temperatures (i.e., 15, 25, 40, and 50 °C). Effect of solution pH was investigated by adjusting solution initial pH from 2.0 to 12.0 using HCl and NaOH solutions with initial F^- concentration of 5 mg/L at 25 °C. To determine the effect of competitive anions on F^- adsorption, batch tests were performed using 5.0 mg/L F^- solutions containing 50, 100, 200, and 500 mg/L of PO_4^{2-}, NO_3^-, SO_4^{2-} or Cl^-, separately. After a 12 h reaction time, the suspension was centrifuged and filtered through a 0.45 μm cellulose acetate filter and analyzed for F^-.

2.3. Analytical methods

Plus benchtop pH/ISE meter (Orion, 4-Star), combined with fluoride electrode (Orion, 9606BNWP), was used for F^- measurement. An approved ASTM method (ASTM D 1179-04) was employed for determination of F^- concentration. Standard pH meter (Sartorius, PB-10) was used for pH determination. The mineral composition of the pristine and used adsorbents was determined by X-ray diffraction (XRD) analysis, using a URD-6 powder diffractometer (Co Kα radiation, graphite monochromator, 2θ range 2.6–70°, step 0.01°, counting time 5 s per step). Morphological analysis of the pristine and used adsorbents was performed by scanning electron microscopy (SEM) using Zeiss SUPRA 55 microscope (at 15 kV) with energy-dispersive X-ray analyses.

3. Results and discussion

3.1. Effect of adsorbent dosage

Effect of adsorbent dosage on F^- adsorption was investigated with adsorbent dosages between 4 and 40 g/L, initial F^- concentration of 20 mg/L, and contact time of 8 h at 25 °C. The results are presented in Fig. 1. The solid line and the dash line shown in Fig. 1 denote the percentage of F^- removal and adsorption capacity (q_t) varying with adsorbent dosage, respectively. The adsorption

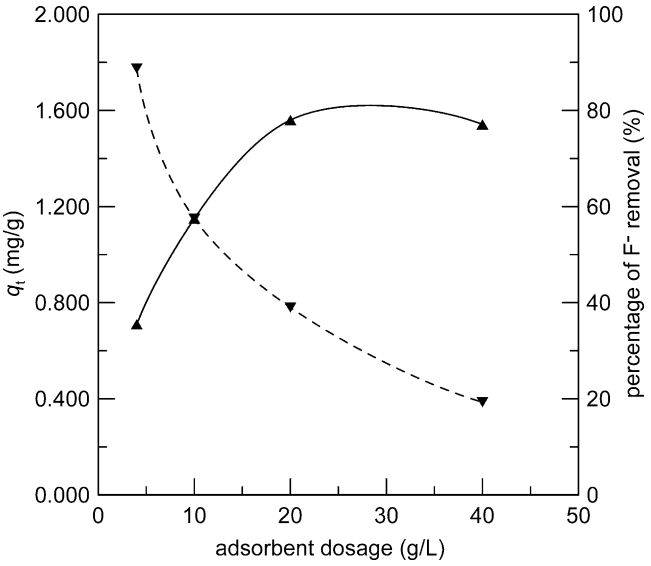

Fig. 1. Effect of adsorbent dosage on percentage of removal and adsorption capacity of F^- (adsorbent dosage = 4–40 g/L, initial F^- concentration = 20 mg/L, T = 25 °C, contact time = 8 h. The solid and dash lines denote the percentage of F^- removal and adsorption capacity (q_t) varying with adsorbent dosage, respectively).

capacity was up to 1.775 mg/g in the batch with an adsorbent dosage of 4 g/L and an initial F^- concentration of 20 mg/L. It can be clearly seen that the amount of adsorbent significantly influenced F^- adsorption. High adsorbent dosage did result in low q_t value at the same initial F^- concentration. This was consistent with the viewpoint that the surface of adsorbent is composed of heterogeneous sites with a spectrum of binding energies. At low adsorbent dosage, all types of adsorption sites were entirely exposed and quickly saturated by F^- adsorption, showing a high q_t value. But at higher adsorbent dosage, the availability of higher energy sites decreased with the increase in the amount of lower energy sites occupied, resulting in a lower q_t value [17].

Furthermore, the percentage of F^- removal significantly increased with the increase in the adsorbent dosage from 4 to 20 g/L. The percentage of F^- removal was 35.5% at 4 g/L of adsorbent dosage, and reached 78.0% at 20 g/L of adsorbent dosage. Therefore, the following experiments were carried out with the adsorbent dosage of 20 g/L.

3.2. Effect of contact time

Effect of contact time on F^- adsorption was carried out with initial F^- concentrations of 3.0 and 20 mg/L at 25 °C. The results are shown in Fig. 2. With the initial F^- concentration of 3.0 mg/L, the adsorption rate was fast and the adsorption capacity (q_t) reached 0.117 mg/g in the first 2 h. With the increase in contact time, the adsorption rate decreased and the adsorption gradually achieved equilibrium at about 12 h. The equilibrium adsorption capacity reached 0.130 mg/g. The same trend was found at the initial F^- concentration of 20 mg/L.

In order to investigate the mechanism of adsorption, two kinetic models, namely, the pseudo-first order model and the pseudo-second order model, were employed. The model equations are presented as follows [22,23]:

$$\ln(q_e - q_t) = \ln q_e - k_1 t \quad (1)$$

$$\frac{t}{q_t} = \frac{1}{k_2 q_2^2} + \frac{t}{q_2} \quad (2)$$

where q_e is the equilibrium adsorption capacity (mg/g), q_2 is the equilibrium adsorption capacity of theoretical value in the pseudo-

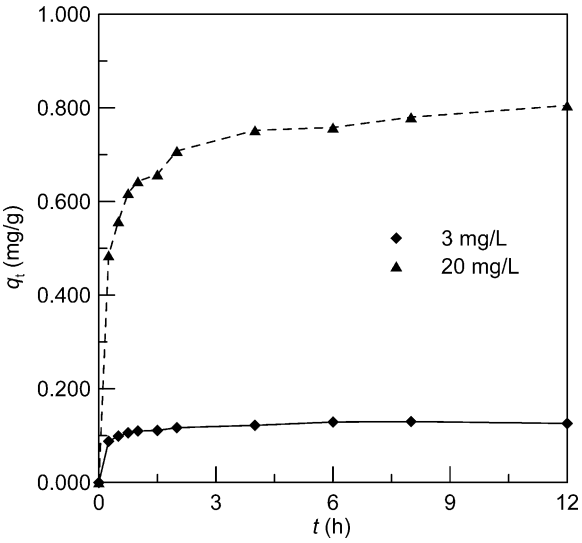

Fig. 2. Effect of contact time on F^- adsorption (adsorbent dosage = 20 g/L, initial F^- concentration = 3 and 20 mg/L, T = 25 °C).

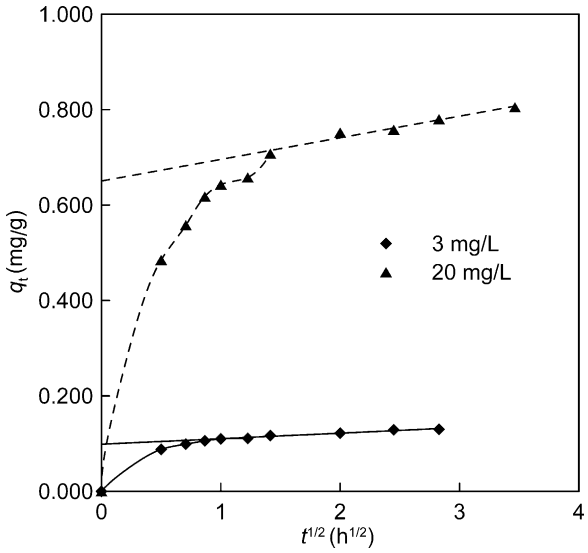

Fig. 3. The curves of intraparticle diffusion for F^- adsorption (adsorbent dosage = 20 g/L, initial F^- concentration = 3 and 20 mg/L, T = 25 °C).

second order model (mg/g), k_1 (h^{-1}) and k_2 (g/(mg h)) are the rate constant of pseudo-first order model and pseudo-second order model, respectively.

The kinetic parameters had been obtained from the straight line fitting the plot of $\ln(q_e - q_t)$ against t or the plot of t/q_t against t (Table 1). It was found that the pseudo-second order model produced a higher correlation coefficient ($R^2 > 0.999$) than the pseudo-first order model for both initial F^- concentrations, which means that the adsorption of F^- on synthetic siderite fitted the pseudo-second order model better.

In most cases, the adsorption of F^- onto solid particles normally takes three general stages: firstly, transport of F^- to the external surface of the adsorbent from bulk solution across the boundary layer surrounding the adsorbent particle, i.e., external mass transfer; secondly, adsorption of F^- onto particle surfaces, which always happens very fast; lastly, exchange of the adsorbed F^- with the structural elements of adsorbent particles, or diffusion of F^- in the internal surfaces of porous materials (intraparticle diffusion). Of these three steps, the slowest one which determines the overall adsorption rate calls "rate-determining step" [24]. Therefore, it is important to investigate whether the intraparticle diffusion is the rate-determining step in adsorption process by using the intraparticle diffusion model (Eq. (3))

$$q_t = K_p t^{1/2} \tag{3}$$

where K_p is the rate constant of intraparticle diffusion (mg/(g $h^{1/2}$)).

The value of q_t was plotted versus the square root of t (Fig. 3). If the intraparticle diffusion is a rate-determining step, the plot should be linear and pass through the origin. However, it can be seen from Fig. 3 that the initial curves were followed by straight lines for both initial concentrations. The initial curve showed external mass transfer, while the straight line indicated intraparticle diffusion. However, the linear portions did not pass the origin in Fig. 3. It indicates that mechanisms of F^- removal by synthetic siderite were complex, and the intraparticle diffusion was not the only rate determining step. Similar dual nature of intraparticle diffusion curve was found for adsorption of F^- onto activated carbon derived from rice straw [25].

Table 2
Effect of initial F^- concentration on adsorption at 15 °C (adsorbent dosage = 20 g/L, contact time = 12 h).

c_0 (mg/L)	c_e (mg/L)	q_e (mg/g)	Percentage of F^- removal (%)
3	0.260	0.1370	91.3
5	0.565	0.2218	88.7
10	1.620	0.4190	83.8
15	2.465	0.6268	83.6
20	3.575	0.8213	82.1

3.3. Effect of initial F^- concentration

Effect of initial F^- concentration was tested with initial F^- concentrations between 3 and 20 mg/L, adsorbent dosage of 20 g/L, and contact time of 12 h at 15, 25, 40, and 50 °C. Table 2 shows the effect of initial F^- concentration on adsorption at 15 °C. With the increase in initial F^- concentration (c_0) from 3 to 20 mg/L, both F^- equilibrium concentration (c_e) and equilibrium adsorption capacity (q_e) exhibited increasing trends. These phenomena were the results of the increase in the driving force provided by the concentration gradient with the increase in the initial F^- concentration (c_0). In contrast, the percentage of F^- removal displayed a decreasing trend. Most F^- interacted with the binding sites at low initial F^- concentration, causing the high percentage of F^- removal, while only part of F^- combined with the finite binding sites at high initial F^- concentration, resulting in the relatively low percentage [26]. In addition, effects of initial F^- concentration on adsorption at other reaction temperatures exhibit the similar trends as those at 15 °C.

Table 1
Parameters of kinetics at different initial F^- concentrations (adsorbent dosage = 20 g/L, T = 25 °C).

c_0 (mg/L)	Pseudo-first order equation		Pseudo-second order equation			Intraparticle diffusion	
	k_1 (h^{-1})	R^2	k_2 (g/(mg h))	q_2 (mg/g)	R^2	K_p (mg/(g $h^{1/2}$))	R^2
3	0.578	0.8828	34.6	0.133	0.9993	0.0117	0.9431
20	0.342	0.8304	4.34	0.814	0.9994	0.0455	0.9635

The equilibrium isotherm models would help to reveal the adsorption mechanism, the surface properties and affinity of the adsorbent. The experimental data of equilibrium isotherm for F^- ions onto synthetic siderite were modeled using the most frequently used Langmuir, Freundlich, and Redlich–Peterson isotherms [27,28]. The Langmuir model is probably the best known and most widely used adsorption isotherm, which is valid for monolayer adsorption onto a surface with the finite number of identical sites [29]. The Freundlich isotherm is an empirical model, which can be applied to nonideal adsorption on heterogeneous surfaces as well as multilayer adsorption [27]. The Redlich–Peterson isotherm incorporates features of both Langmuir and Freundlich equations. Three models are described as follows:

$$q_e = \frac{q^0 b c_e}{(1 + b c_e)} \tag{4}$$

$$q_e = k c_e^{1/n} \tag{5}$$

$$q_e = \frac{A c_e}{(1 + B c_e^g)} \tag{6}$$

where c_e is the equilibrium concentration of F^- in aqueous phase (mg/L); q_e is the amount adsorbed on the adsorbent at equilibrium (mg/g); q^0 and b are the maximum adsorption capacity (mg/g) and adsorption equilibrium constant (L/mg) in Langmuir isotherms, respectively; k and $1/n$ are empirical constants of Freundlich isotherms, indicating the adsorption capacity and adsorption intensity, respectively; Redlich–Peterson isotherm has three isotherm constants, namely, A, B, and g ($0 < g < 1$).

Eqs. (4) and (5) have been converted to linear forms, as shown in Eqs. (7) and (8)

$$\frac{c_e}{q_e} = \frac{1}{q^0 b} + \frac{c_e}{q^0} \tag{7}$$

$$\ln q_e = \ln k + \ln c_e / n \tag{8}$$

The constants of Langmuir and Freundlich isotherms can be calculated from the slope and the intercept of the isotherm plots. Three isotherm constants A, B, and g in Redlich–Peterson isotherm can be evaluated by using a mathematical software called Matlab to maximize correlation coefficient (R^2).

All the adsorption data obtained were fitted to three models. The plots of Langmuir and Freundlich isotherms are shown in Fig. 4. The correlation coefficients and constants for Langmuir, Freundlich, and Redlich–Peterson isotherms at various temperatures are summarized in Table 3. It was observed that there were higher correlation coefficients for both Freundlich and Redlich–Peterson isotherms than Langmuir isotherm, indicating that F^- adsorption closer followed Freundlich and Redlich–Peterson isotherms. Therefore, it suggests that the multilayer adsorption should be involved in the process of F^- removal by the synthetic siderite with heterogeneous surfaces.

Table 3
Isotherm parameters at different temperatures.

Isotherm		T (°C)			
		15	25	40	50
Langmuir	b (L/mg)	0.3341	0.2027	0.1558	0.0457
	q^0 (mg/g)	1.413	1.713	1.833	3.792
	R^2	0.8582	0.9057	0.9959	0.7662
Freundlich	k (mg/g) $(L/mg)^{1/n}$	0.3308	0.2761	0.2382	0.1666
	n	1.473	1.312	1.256	1.110
	R^2	0.9944	0.9956	0.9963	0.9986
Redlich–Peterson	g	0.2682	0.2314	0.7965	0.2142
	A (L/g)	16.18	4.976	0.3103	0.2439
	B $(L/mg)^g$	49.81	17.22	0.2530	0.4963
	R^2	0.9940	0.9965	0.9997	0.9979

3.4. Thermodynamic study

It is necessary to evaluate the thermodynamic feasibility and to confirm the nature of the adsorption process based on the determination of thermodynamic parameters. The Gibbs free energy change (ΔG^o in kJ/mol), is an indication of spontaneity of a reaction. It can be given by the following equation in terms of K_c, the adsorption equilibrium constant [29,30]:

$$\Delta G^o = -RT \ln K_c \tag{9}$$

$$K_c = \frac{c_{Ae}}{c_e} \tag{10}$$

where R is the universal gas constant (8.314 J/mol K); T is absolute temperature (K); K_c is the adsorption equilibrium constant; c_{Ae} is the equilibrium concentration on the adsorbent (mg/L).

The relationship among ΔG^o, enthalpy change (ΔH^o in kJ/mol) and entropy change (ΔS^o in kJ/(mol K)) can be presented as follows:

$$\Delta G^o = \Delta H^o - T\Delta S^o \tag{11}$$

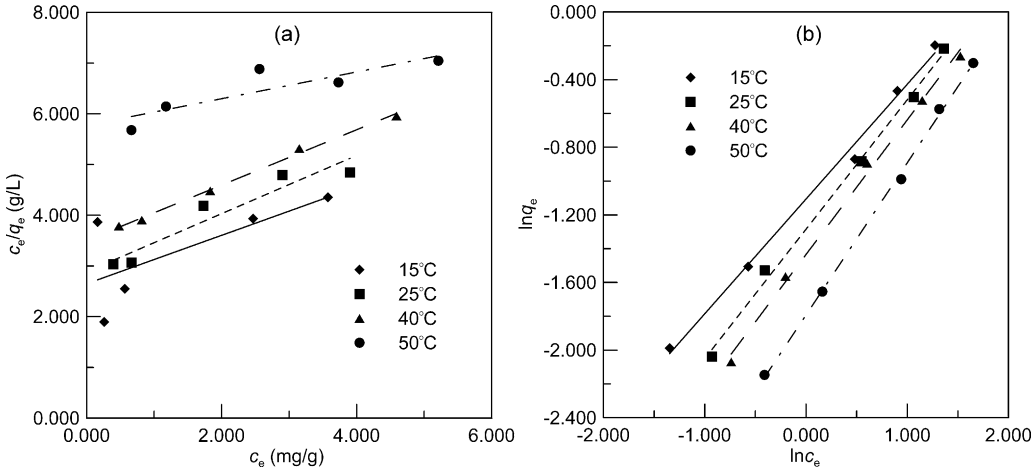

Fig. 4. Langmuir(a) and Freundlich (b) isotherms of F^- adsorption on synthetic siderite at different temperatures (adsorbent dosage = 20 g/L, initial F^- concentration = 3–20 mg/L, T = 15–50 °C, contact time = 12 h).

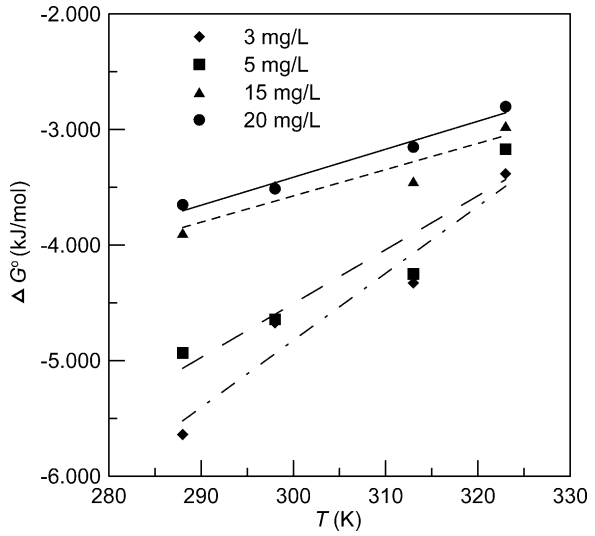

Fig. 5. Plot of Gibbs free energy change (ΔG^o) vs. temperature (T) (adsorbent dosage = 20 g/L, initial F^- concentration = 3–20 mg/L, T = 15–50 °C, contact time = 12 h).

A plot of Gibbs free energy change (ΔG^o) versus temperature (T) is shown in Fig. 5. It was found that there is a good linear relationship between ΔG^o and T. The values of ΔH^o and ΔS^o were determined from the slopes and intercepts of the fitting lines.

Thermodynamic parameters for the adsorption of F^- on synthetic siderite are listed in Table 4. The values of ΔG^o calculated using the K_a were negative, which confirm the feasibility of the process and the spontaneous nature of the adsorption. The increase in the negative value of ΔG^o with the increase in temperature at the fixed initial F^- concentration indicates that the adsorption process of F^- onto synthetic siderite became less favorable at higher temperature [31,32]. The negative values of ΔH^o denote that the process was exothermic. The exothermic nature may also be predicted from the decrease in the adsorption capacity calculated by Freundlich model with the increase in reaction temperature (Table 3). Generally, adsorption processes were associated with positive values of ΔS^o. However, the negative values of ΔS^o were observed in this study, which generally increased with the increase in initial F^- concentration (Table 4). Sarkar et al. [33] has also observed the spontaneous and exothermic adsorption with negative ΔS^o values when they investigated the F^- adsorption on laterite.

Table 4
Thermodynamic parameters of F^- adsorption on synthetic siderite.

c_0 (mg/L)	T (°C)	ΔG^o (kJ/mol)	ΔS^o (kJ/(mol K))	ΔH^o (kJ/mol)
3	15	−5.639	−0.0581	−22.252
	25	−4.673		
	40	−4.328		
	50	−3.383		
5	15	−4.934	−0.0458	−18.24
	25	−4.645		
	40	−4.250		
	50	−3.170		
15	15	−3.894	−0.0227	−10.375
	25	−3.487		
	40	−3.448		
	50	−2.969		
20	15	−3.651	−0.024	−10.61
	25	−3.513		
	40	−3.152		
	50	−2.802		

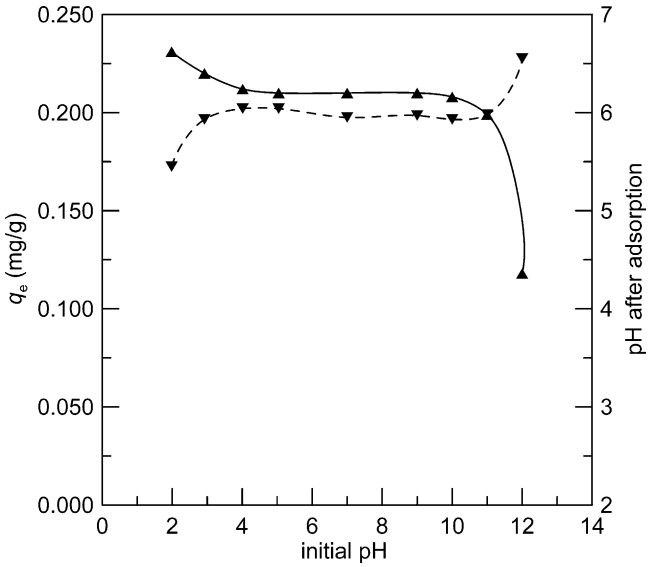

Fig. 6. Effect of initial solution pH on F^- adsorption (adsorbent dosage = 20 g/L, initial F^- concentration = 5 mg/L, T = 25 °C, initial solution pH = 2.0–12.0, contact time = 12 h. The solid and dash lines denote the equilibrium adsorption capacity (q_e) and pH after adsorption, respectively).

3.5. Effect of solution pH

Effect of initial solution pH on F^- adsorption was carried out by using F^- solutions with various initial pHs between 2.0 and 12.0. The results are shown in Fig. 6. The equilibrium adsorption capacity (q_e) kept a relatively constant value for F^- solutions with initial pHs 4–10, although it generally decreased with the increase in initial solution pH. The q_e value was 0.231 mg/g in the batch with initial solution pH of 2, which decreased to 0.210 mg/g with initial pH of 4. Importantly, the values held relatively stable at initial pHs 4–10, which is of great importance for practice application. However, the equilibrium adsorption capacity significantly declined at initial pHs > 10.

Moreover, when the initial solution pH was in the range of 4–11, the pH values after adsorption were about 6.2. It means that the adsorbent had capability in maintaining a neutral solution pH and kept the adsorption system at near neutral pH during the experiments. This broad optimum pH could be explained by the amphoteric nature of Fe oxides/oxyhydroxides [16], since Fe hydroxide minerals mainly attributed to F^- removal (which will be discussed later).

3.6. Effect of coexisting anions

The F^--contaminated drinking water always contains other anions, which can compete for adsorption sites in the adsorption process. In order to study the effect of coexisting ions, the adsorption studies were investigated with initial F^- concentration of 5 mg/L in the presence of different concentrations of Cl^-, NO_3^-, SO_4^{2-}, or PO_4^{3-}, separately. The effect of the anions on F^- removal is shown in Fig. 7, where c_a denotes the initial concentration of coexisting anions. The adverse effect of the anion on F^- removal increased in the following order: $Cl^- < NO_3^- < SO_4^{2-} < PO_4^{3-}$. The former two anions had practically less effect on F^- adsorption. By contrast, PO_4^{3-} showed considerably negative effect on F^- removal. In addition, higher concentrations of coexisting anions occupied more active sites, and brought about more powerful competitive adsorptions, which could result in a decline in adsorption capacity for F^- [13].

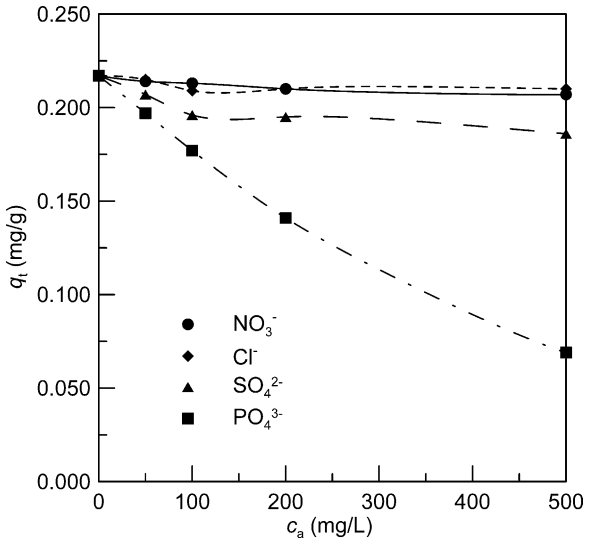

Fig. 7. Effect of coexisting anions on F^- adsorption (adsorbent dosage = 20 g/L, initial F^- concentration = 5 mg/L, T = 25 °C, contact time = 12 h, initial anion concentrations = 50–500 mg/L; c_a denotes the initial concentration of coexisting anions).

3.7. Mechanisms of fluoride removal

Pristine synthetic siderite is a brownish green material with a poorly crystalline structure. From the XRD pattern in Fig. 8a, it can be seen that siderite was the predominant mineral in the pristine synthetic siderite. After F^- adsorption, siderite was partially changed into goethite (Fig. 8b), which is a hydrous iron oxide mineral with a very high affinity for F^- [13]. Hiemstra and Van Riemsdijk found that F^- exchange against either the singly coordinated surface hydroxyls of goethite or the doubly coordinated OH groups, depending on the F^- initial concentrations [35].

The SEM images also show that pristine synthetic siderite changed the mineral phase during the adsorption (Fig. 9). There were many spherical particles (~200 nm diameter) presented in the pristine adsorbent (Fig. 9a), whereas after adsorption, needle-like goethite was covered on surface of the adsorbent (Fig. 9b), which drastically enhanced the specific surface area. The same change was observed when the synthetic siderite and the natural siderite were used to remove As from aqueous solution [16,34].

Therefore, the high removal efficiency of synthetic siderite possibly attributed to adsorption of F^- on the fresh goethite with large specific surface area. In addition, coprecipitation of ferric

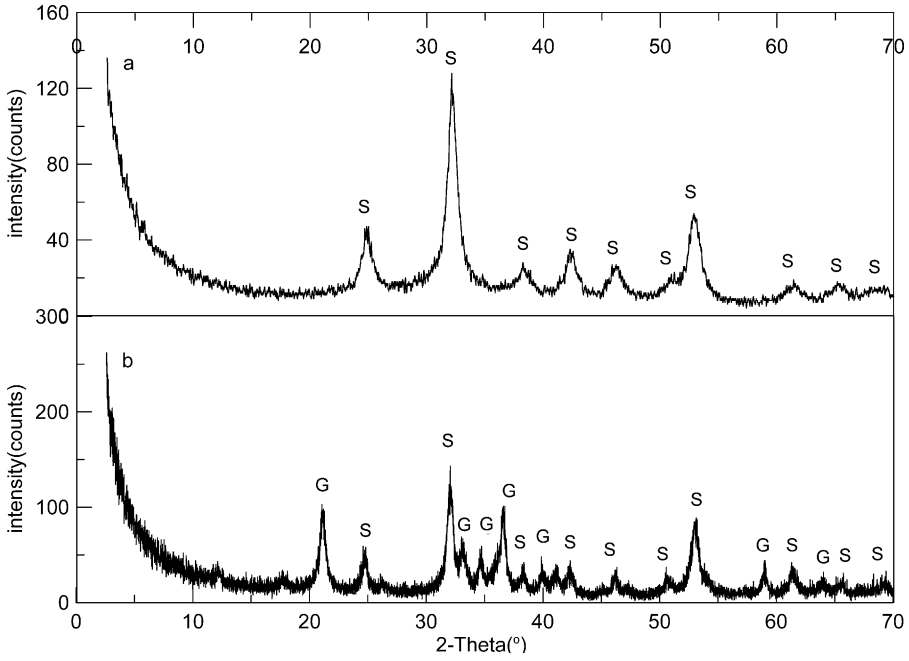

Fig. 8. XRD patterns of the pristine adsorbent (a) and the used adsorbent (b) (S and G represent siderite and goethite, respectively).

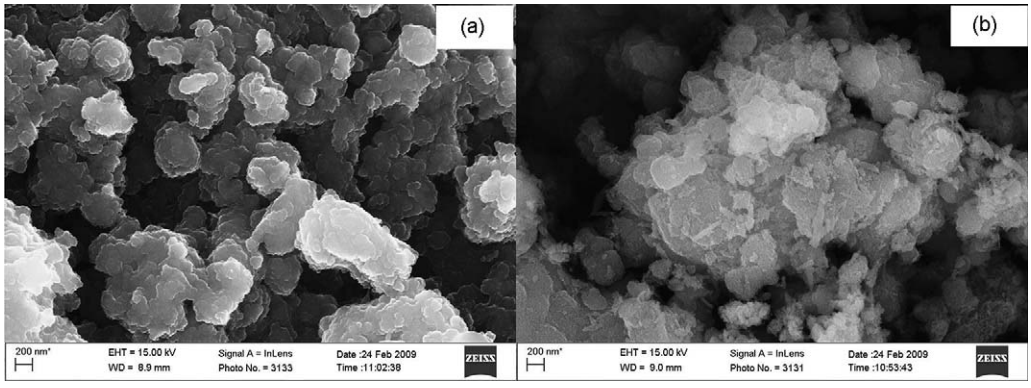

Fig. 9. SEM images of the pristine adsorbent (a) and the used adsorbent (b).

hydroxide with F^-, which was caused by dissolution of pristine synthetic siderite and subsequent oxidization of Fe^{2+}, could also contribute to the fixation of F^- on the adsorbent.

4. Conclusion

Fluoride adsorption on the synthetic siderite significantly increased with an increase in contact time. The adsorption rate was high in the first 2 h, and thereafter significantly decreased until adsorption reached equilibrium. Kinetic data were well fitted to a pseudo-second order kinetic model. It shows that adsorption was controlled by both external mass transfer and intraparticle diffusion. The adsorption closely followed Freundlich and Redlich–Peterson isotherms, which indicates that the multilayer adsorption was involved in the process of F^- removal. Fluoride adsorption capacity decreased with an increase in reaction temperature, suggesting that F^- adsorption on synthetic siderite was exothermic in nature. Fluoride removal was proved to be independent on initial pHs between 4 and 9. The presence of Cl^- and NO_3^- had less effect on F^- adsorption, while SO_4^{2-} and PO_4^{3-} negatively affected F^- removal from aqueous solution. High F^- adsorption capacity on synthetic siderite was believed to result from both coprecipitation of ferric hydroxide with F^- and adsorption of F^- on fresh goethite during the adsorption process.

Acknowledgements

The study is financially supported by National Natural Science Foundation of China (Nos. 40572145 and 40872160), National Special Program on Control and Treatment of Water Pollution (No. 2008ZX07425-06), the Program for New Century Excellent Talents in University (No. NCET-07-0770), and the National Key-technologies R&D Program (No. 2006BAJ08B04) of the 11th 5-year Plan of the People's Republic of China. The authors are grateful to Li Yuan, Wei Chao, Zhao Kai and Zhang Bo for their experimental assistance.

References

[1] R.C. Meenakshi, Msheshwari, J. Hazard. Mater. 137 (2006) 456–463.
[2] G.X. Wang, G.D. Cheng, Scientia. Geographica Sinca 20 (2) (2000) 153–159.
[3] K. Biswas, K. Gupta, U.C. Ghosh, Chem. Engin. J. 149 (2009) 196–206.
[4] M. Mahramanlioglu, I. Kizilcikli, I.O. Bicer, J. Fluorine Chem. 115 (2002) 41–47.
[5] WHO, 2006. Guidelines for drinking-water quality, incorporating 1st and 2nd addenda, vol. 1, 3rd edition. http://www.who.int/water_sanitation_health/dwq/fulltext.pdf.
[6] Ministry of Health of PR China. Standards for drinking water quality, GB5749-2006, 2006.
[7] M. Arora, R.C. Maheshwari, S.K. Jain, A. Gupta, Desalination 170 (2) (2004) 105–112.
[8] E. Ergun, A. Tor, Y. Cengeloglu, I. Kocak, Sep. Purif. Technol. 64 (2008) 147–153.
[9] M.M. Emamjomeh, M. Sivakumar, J. Environ. Manage. 90 (2009) 1663–1679.
[10] S.M. Maliyekkal, S. Shukla, L. Philip, I.M. Nambi, Chem. Eng. J. 140 (2008) 183–192.
[11] E. Kumar, A. Bhatnagar, M. Ji, W. Jung, S.H. Lee, S.J. Kim, G. Lee, H. Song, J.Y. Choi, J.S. Yang, B.H. Jeon, Water Res. 43 (2009) 490–498.
[12] G. Lee, C. Chen, S.T. Yang, W.S. Ahn, Micropor. Mesopor. Mater. 127 (2010) 152–156.
[13] H.M. Guo, Q. Liu, J. Safety Environ. 8 (2) (2008) 26–30.
[14] H. Xie, W. Jia, Z. Wu, Acta Medicinae Universitatis Scientiae et Technologiae Huazhong 34 (5) (2005) 644–646.
[15] M. Karthikeyan, K.K. Satheesh Kumar, K.P. Elango, J. Fluorine Chem. 130 (2009) 894–901.
[16] H.M. Guo, Y. Li, K. Zhao, Y. Ren, J. Hazard. Mater. 176 (2010) 174–180.
[17] X.P. Liao, B. Shi, Environ. Sci. Technol. 39 (2005) 4628–4632.
[18] C.S. Zhu, G.L. Bai, X.L. Liu, Y. Li, Water Res. 41 (2007) 1168–11168.
[19] M.A. Armienta, N. Segovia, Environ. Geochem. Health 30 (2008) 345–353.
[20] A. Farooqi, H. Masuda, R. Siddiqui, M. Naseem, Environ. Contam. Toxicol. 56 (2009) 693–706.
[21] M.L. Gomez, M.T. Blarasin, D.E. Martinez, Environ. Geol. 57 (2009) 143–155.
[22] X.Y. Yang, B. Al-Duri, J. Colloid Interf. Sci. 287 (2005) 25–34.
[23] Y.S. Ho, G. McKay, Process Biochem. 34 (1999) 451–465.
[24] X. Fan, D.J. Parker, M.D. Smith, Water Res. 37 (2003) 4929–4937.
[25] A.A.M. Daifullah, S.M. Yakout, S.A. Elreefy, J. Hazard. Mater. 147 (2007) 633–643.
[26] A. Özer, D. Özer, A. Özer, Process Biochem. 39 (2004) 2183–2191.
[27] Y.S. Ho, A.E. Ofomaja, Biochem. Eng. J. 30 (2006) 117–123.
[28] S. Hong, C. Wen, J. He, F. Gan, Y.S. Ho, J. Hazard. Mater. 167 (2009) 630–633.
[29] M. Islam, R. Patel, J. Hazard. Mater. 156 (2008) 509–520.
[30] M.G. Sujana, H.K. Pradhan, S. Anand, J. Hazard. Mater. 161 (2009) 120–125.
[31] G.F. Hülya, T.C. Jens, M. David, Environ. Sci. Technol. 38 (8) (2004) 2428–2434.
[32] V.K. Gupta, I. Ali, V.K. Saini, Water Res. 41 (2007) 3307–3316.
[33] M. Sarkar, A. Banerjee, P.P. Pramanick, A.R. Sarkar, J. Colloid Interf. Sci. 302 (2006) 432–441.
[34] H.M. Guo, D. Stüben, Z. Berner, J. Colloid Interf. Sci. 315 (2007) 47–53.
[35] T. Hiemstra, W.H. Van Riemsdijk, J. Colloid Interface Sci. 225 (2000) 94–104.